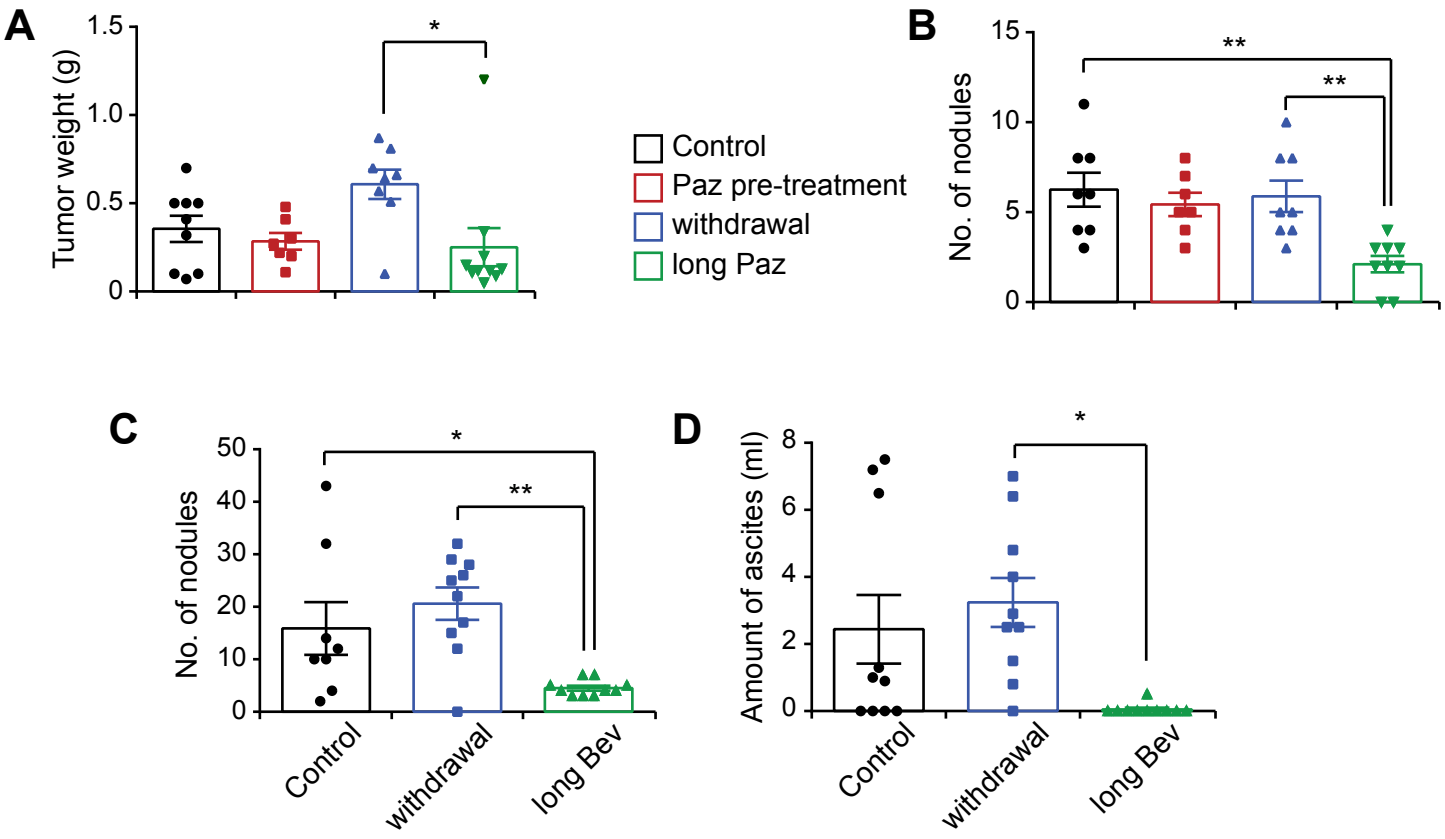

Supplemental Figure 1. Effect of withdrawal versus long-term anti-angiogenic therapy. Mean aggregate tumor weight (**A**) and number of tumor nodules (**B**) of tumors induced by intra-peritoneal injection of HeyA8 human ovarian cancer cells into nude mice after indicated treatments. Number of tumor nodules (**C**) and amount of ascites in ml (**D**) of 2774 intraperitoneal tumors after withdrawal or long-term treatment with bevacizumab. (**A-D**) n=8-10 mice per group. ***$P < 0.001$, **$P < 0.01$, *$P < 0.05$ (1-way ANOVA followed by a Tukey's multiple comparison post-hoc test in **A-D**). Averaged data are presented as the mean ±SEM.

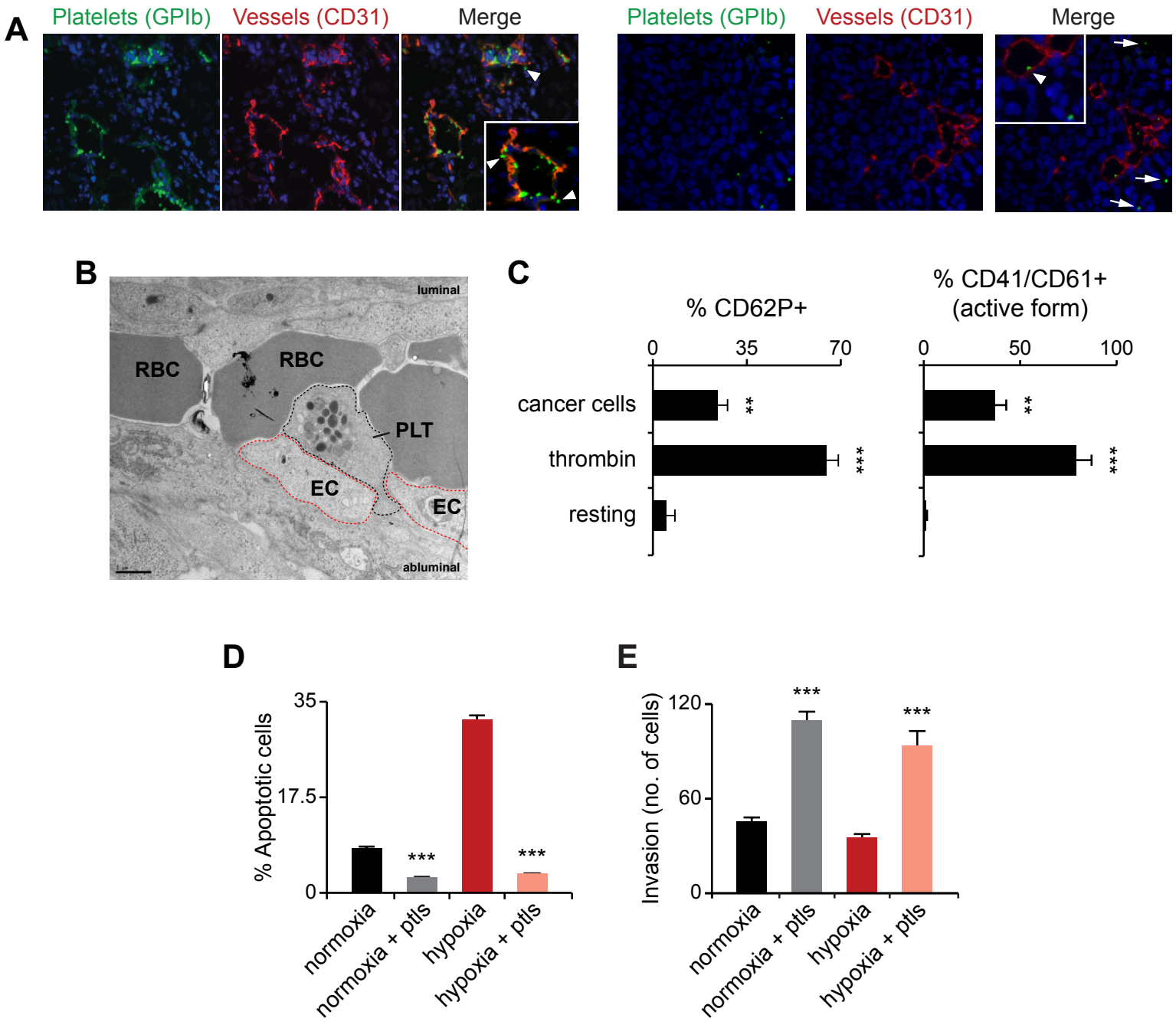

Supplemental Figure 2. Platelet infiltration in vivo and platelet effect on cancer cells in vitro. (**A**) Higher magnification of respresentative tumor sections showing platelets attached to the vessel wall and at the point of extravasation (white arrowheads) or extravasated (white arrows) into tumor micro-environment. Platelets and tumor vessels were stained with antibodies against GPIb and CD31, respectively. Representative pictures of tumors from at least 5 mice per group. (**B**) Electron microscopy picture of a platelet (PLT - black dashed line) extravasating between two endothelial cells (EC, red dashed line). RBC=red blood cell. Scale bar 1µm. Representative picture of tumors from at least 5 mice. (**C**) Evaluation of P-selectin and CD41/CD61 (active form) surface expression in GPIbβ-positive platelets as evidence of platelet activation by cancer cells. Thrombin stimulation (0.5U/ml) of platelets was used as positive control (n=3). (**D**) Number of apoptotic SKOV3 ovarian cancer cells (in %) under normoxic or hypoxic conditions with or without the addition of 20 million platelets (n=3). (**E**) Indirect effect of platelets on SKOV3 invasiveness under normoxic and hypoxic conditions (no. of invaded cells, n=3). ***$P < 0.001$, **$P < 0.01$, *$P < 0.05$ (1-way ANOVA followed by a Dunnett's multiple comparison post-hoc test in **C**; two-tailed Student's t-test in **D-E**). Averaged data are presented as the mean ±SEM.

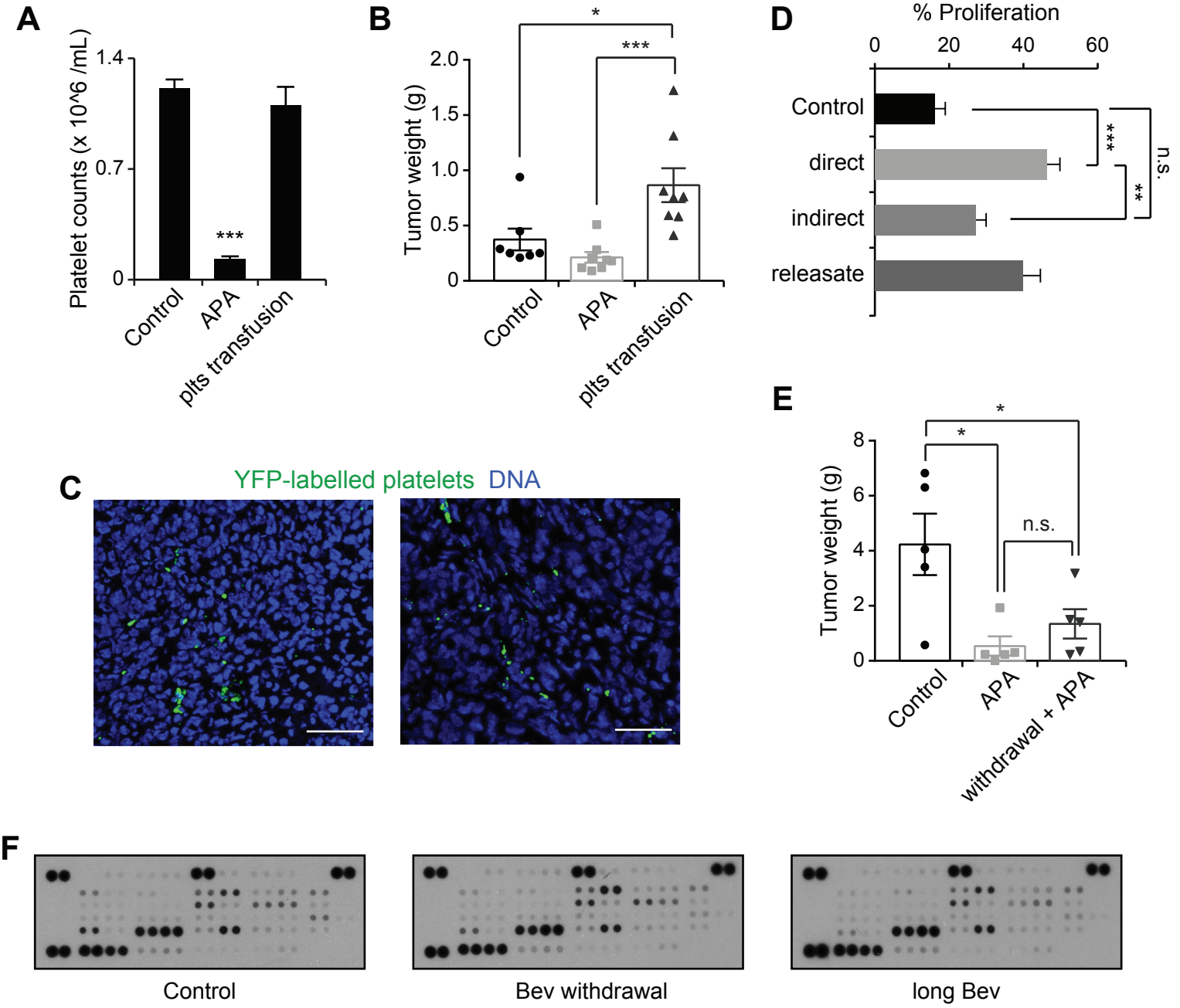

Supplemental Figure 3. Effect of platelets on tumor growth. (**A**) Platelet counts in blood of mice with A2780 intraperitoneal ovarian cancer at the time of necropsy after twice weekly injection with anti-platelet antibody (APA) or platelet transfusions (n=3 mice per group). (**B**) Mean aggregate tumor weight in mice harboring intraperitoneal SKOV3ip1 ovarian tumors after twice weekly injection with APA or platelet transfusions (n=8 mice per group). (**C**) YFP-labelled platelets inside the tumor microenvironment after i.v. transfusion. Scale bar 50μM. Representative images of tumors from at least 5 mice. (**D**) Rate of proliferation of HeyA8 cells in vitro after direct or indirect (with endothelial cell monolayer on transwell as separation) platelet exposure or HeyA8 cells exposed to platelet releasate (n=3). (**E**) Mean aggregate tumor weight of A2780ip2 intraperitoneal tumors in control mice, mice treated with APA (started on day 1) or APA plus one week of bevacizumab with subsequent withdrawal (n=5 per group). (**F**) Mouse angiogenesis array of isolated platelet proteins from A2780ip2 tumor bearing mice of indicated groups (n=2). ***$P < 0.001$, **$P < 0.01$, *$P < 0.05$ (1-way ANOVA followed by a Tukey's multiple comparison post-hoc test in **A, B, D, E**). Averaged data are presented as the mean ±SEM.

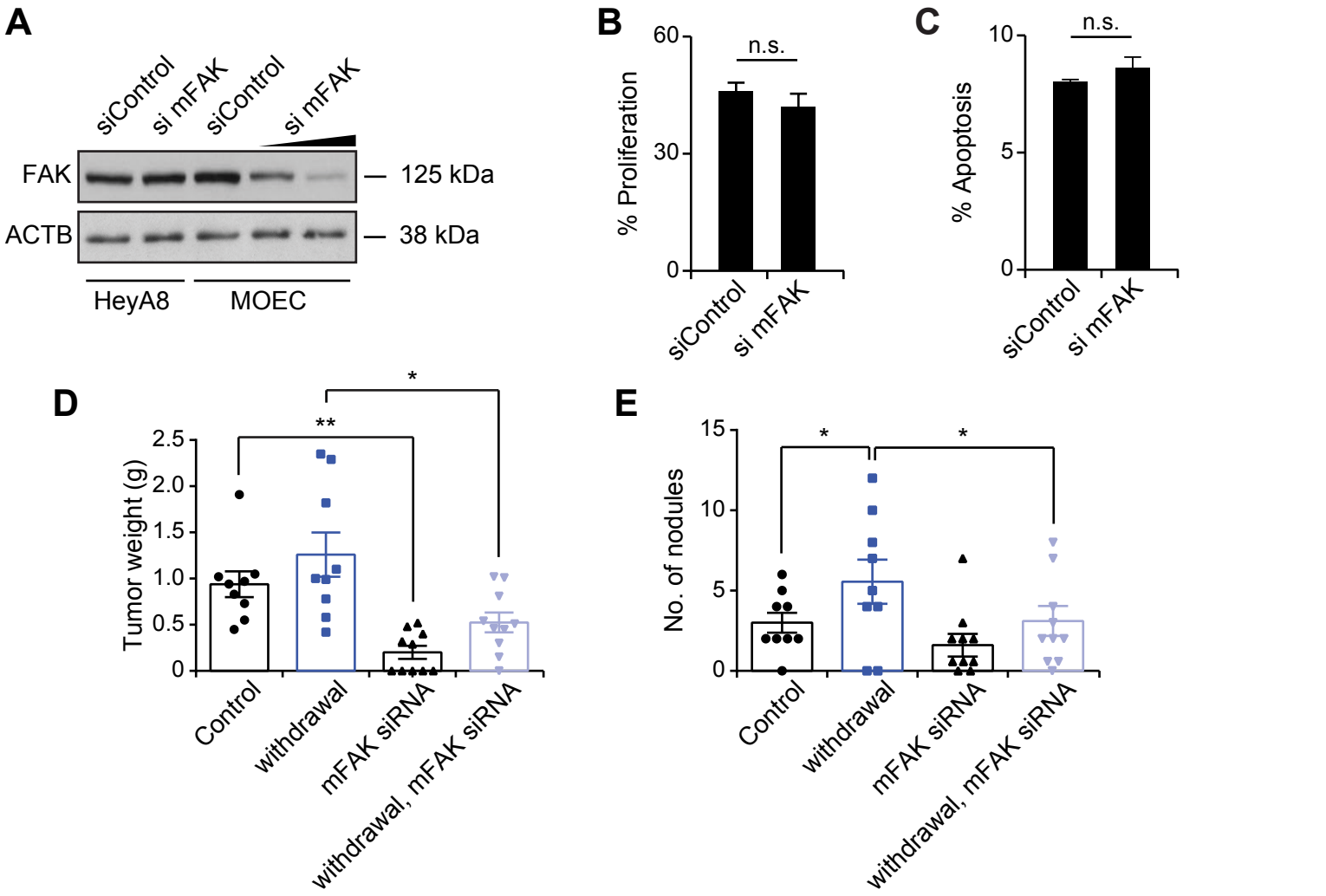

Supplemental Figure 4. siRNA-mediated knockdown of FAK. (**A**) Efficiency of mouse-specific siRNA tested in the human ovarian cancer cell line HeyA8 (100nM f.c.) and mouse ovarian endothelial cells (40nM and 100nM f.c.). Beta-actin was used as loading control (n=2). Proliferation (**B**) and apoptosis (**C**) of HeyA8 cells 48 and 72 hours after transfection of mouse-specific FAK siRNA (n=3). (**D, E**) Mean aggregate tumor weight (**D**) and average number of nodules (**E**) of intraperitoneal HeyA8 tumors after withdrawal of bevacizumab treatment, twice weekly injection of mouse-specific siRNA and combination of both (n=9-10 mice per group). ***$P < 0.001$, **$P < 0.01$, *$P < 0.05$ (two-tailed Student's t-test in **B, C**; 1-way ANOVA followed by a Tukey's multiple comparison post-hoc test in **D, E**). Averaged data are presented as the mean ±SEM.

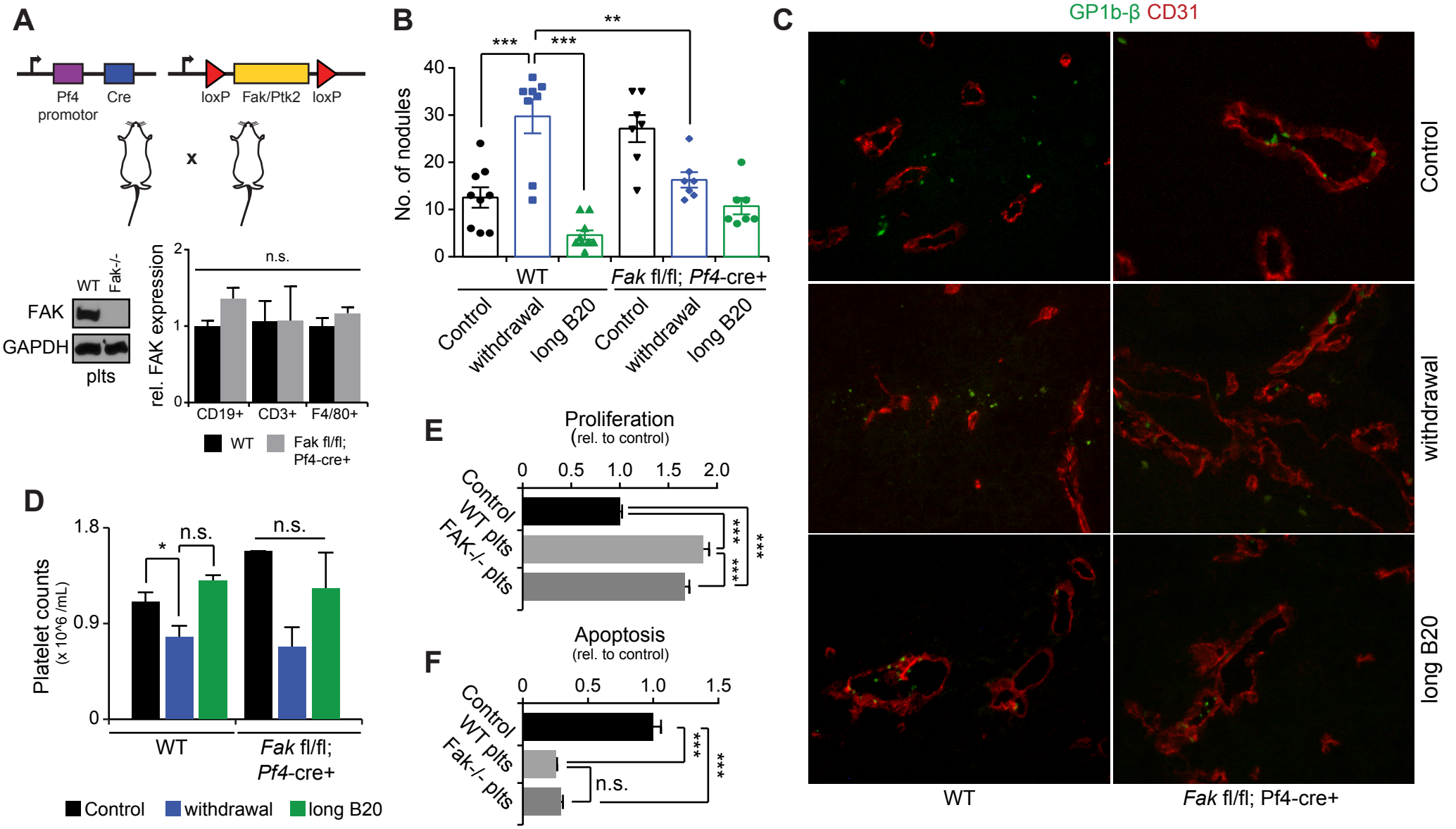

Supplemental Figure 5. Platelet-specific KO of FAK. (**A**) Schema of platelet-specific FAK KO mice using Pf4 as a tissue specific promotor. Validation of absence of FAK expression in platelet protein lysates. qRT-PCR analysis for FAK expression in CD19+ B-cells, CD3+ T-cells and F4/80+ macrophages, isolated from the spleen of WT and *Fak fl/fl; Pf4-cre+* mice (n=2). (**B**) Average number of nodules in WT and *Fak fl/fl;Pf4-cre+* mice after withdrawal or long-term treatment with B20 antibody (7-10 mice per group). (**C**) Extravasated platelets in WT and FAK KO tumors. Representative images of tumors from at least 5 mice per group. (**D**) Platelet counts in WT and KO mice in indicated groups (n=3). (**E**) Proliferation and (**F**) apoptosis rates of ID8-VEGF mouse ovarian cancer cells co-incubation with WT or FAK-/- plts (n=3). ***P < 0.001, **P < 0.01, *P < 0.05 (two-tailed Student's t-test in **A**; 1-way ANOVA followed by a Tukey's multiple comparison post-hoc test in **B, D-F**). Averaged data are presented as the mean ±SEM.

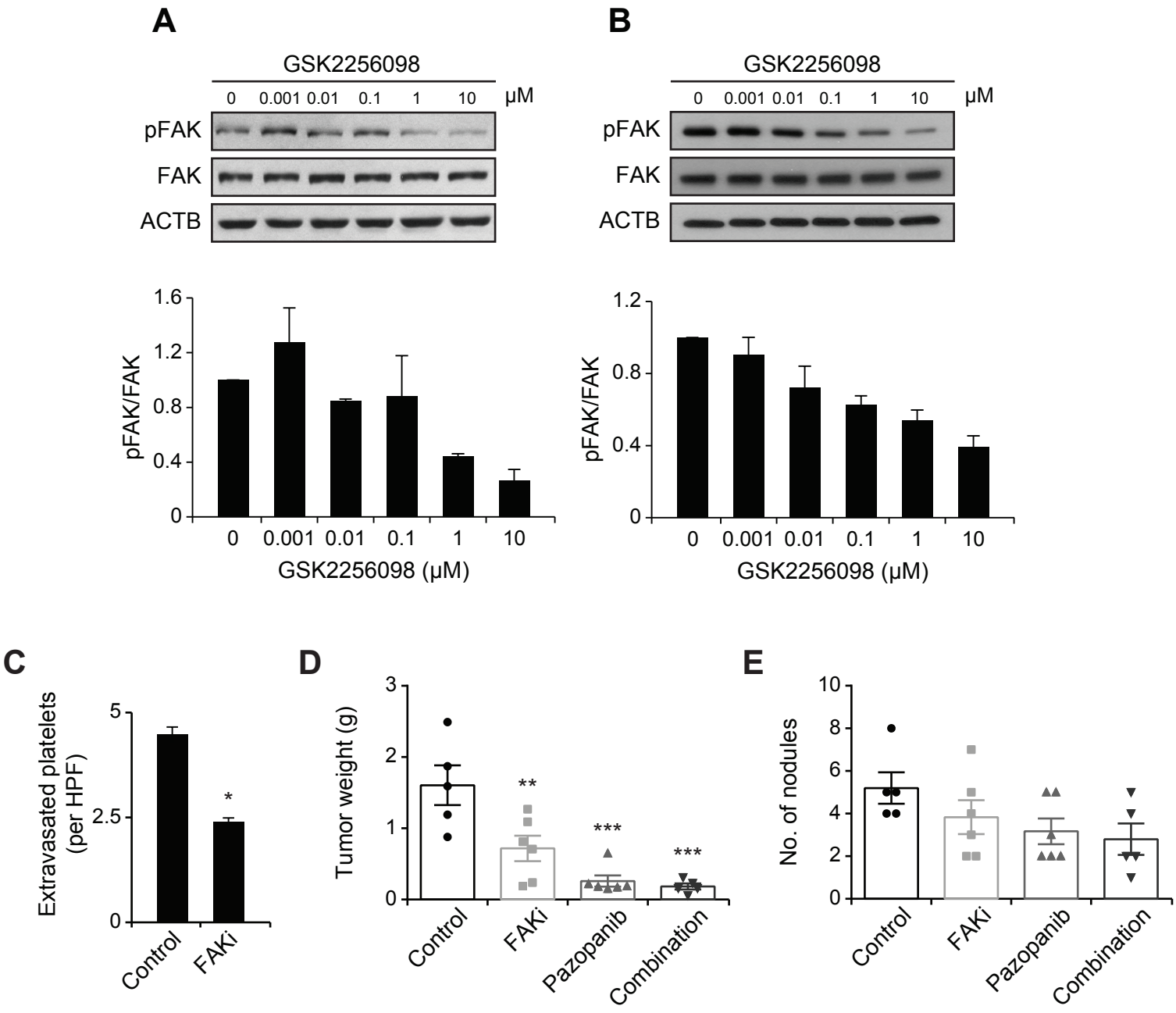

Supplemental Figure 6. Effect of the FAK inhibitor GSK2256098 on ovarian cancer growth. (**A**) Western blot analysis and densitometry for p(Y397) and total FAK in SKOV3ip1 cells treated with GSK2256098 (n=2). β-actin was used as loading control. (**B**) Western blot analysis and densitometry for p(Y397) and total FAK in HeyA8 cells treated with GSK2256098 (n=2). β-actin was used as loading control. (**C**) Number of extravasated platelets in SKOV3ip1 control tumors and tumors treated with GSK2256098 (quantification in tumors of at least 5 mice per group). Mean aggregate tumor weight (**D**) and average number of tumor nodules (**E**) of HeyA8 intraperitoneal tumors after treatment with GSK2256098 (FAKi), pazopanib or a combination of both drugs (n=5-6 mice per group in **D, E**). ***P < 0.001, **P < 0.01, *P < 0.05 (two-tailed Student's t-test in **C**; 1-way ANOVA followed by a Tukey's multiple comparison post-hoc test in **D, E**). Averaged data are presented as the mean ±SEM.

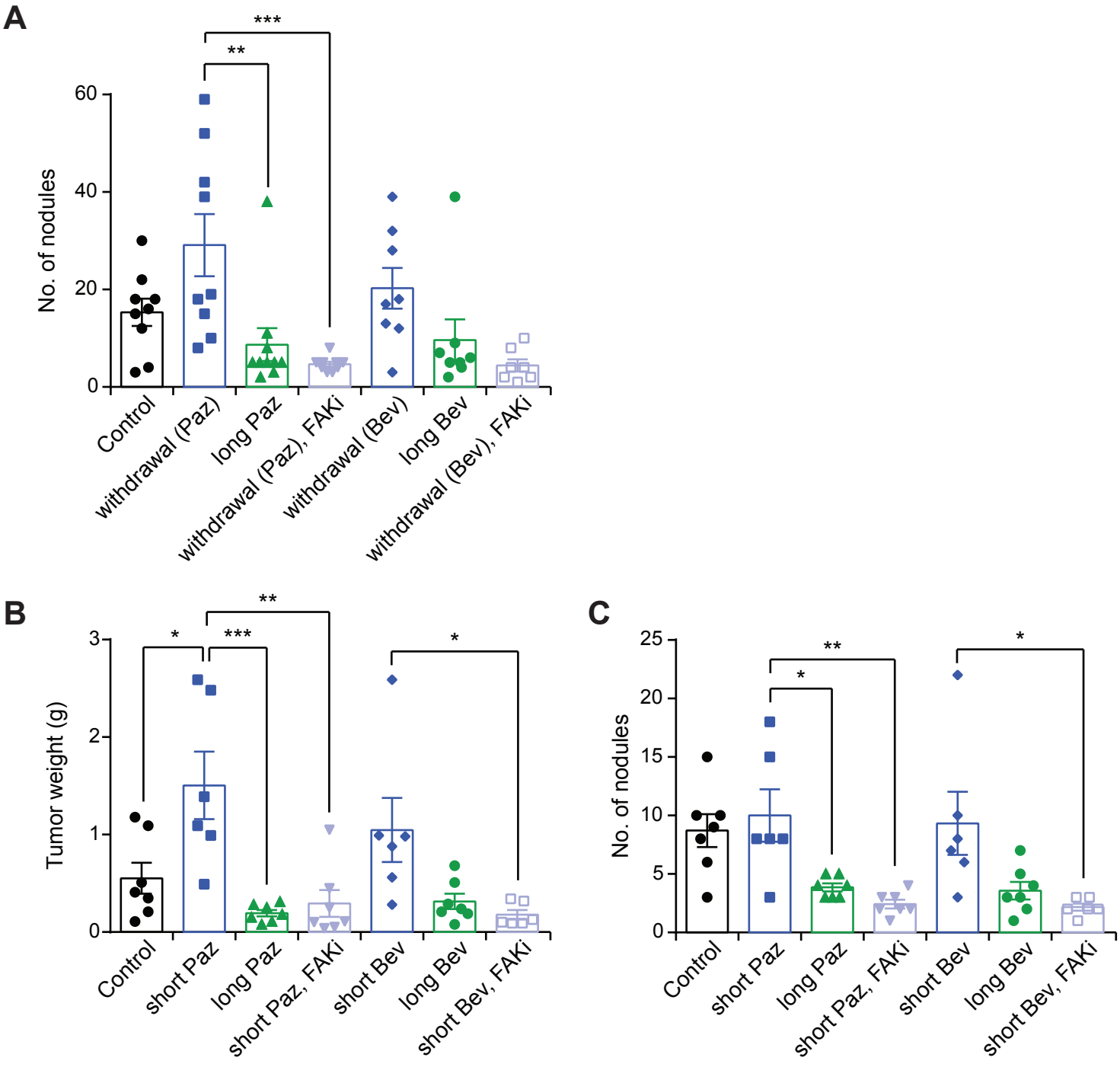

Supplemental Figure 7. Effect of FAK inhibition of tumor outgrowth after withdrawal of anti-angiogenic therapy. (**A**) Average number of nodules of orthotopic SKOV3ip1 tumors after anti-angiogenic therapy (Paz; pazopanib or Bev; bevacizumab) alone or in combination with the FAK inhibitor GSK2250698 (FAKi). Mean aggregate tumor weight (**B**) and average number of tumor nodules (**C**) of orthotopic HeyA8 tumors after anti-angiogenic therapy (Paz; pazopanib or Bev; bevacizumab) alone or in combination with the FAK inhibitor GSK2250698 (FAKi) (n=6-9 mice per group in **A-C**). ***$P < 0.001$, **$P < 0.01$, *$P < 0.05$ (1-way ANOVA followed by a Tukey's multiple comparison post-hoc test in **A-C**). Averaged data are presented as the mean ±SEM.